

Field theory of the inverse cascade in two-dimensional turbulence

Jackson R. Mayo*

Department of Physics, Princeton University, Princeton, New Jersey 08544-0708

A two-dimensional fluid, stirred at high wavenumbers and damped by both viscosity and linear friction, is modeled by a statistical field theory. The fluid's long-distance behavior is studied using renormalization-group (RG) methods, as begun by Forster, Nelson, and Stephen [Phys. Rev. A **16**, 732 (1977)]. With friction, which dissipates energy at low wavenumbers, one expects a stationary inverse energy cascade for strong enough stirring. While such developed turbulence is beyond the quantitative reach of perturbation theory, a combination of exact and perturbative results suggests a coherent picture of the inverse cascade. The zero-friction fluctuation-dissipation theorem (FDT) is derived from a generalized time-reversal symmetry and implies zero anomalous dimension for the velocity even when friction is present. Thus the Kolmogorov scaling of the inverse cascade cannot be explained by any RG fixed point. The β function for the dimensionless coupling \hat{g} is computed through two loops; the \hat{g}^3 term is positive, as already known, but the \hat{g}^5 term is negative. An ideal cascade requires a linear β function for large \hat{g} , consistent with a Padé approximant to the Borel transform. The conjecture that the Kolmogorov spectrum arises from an RG flow through large \hat{g} is compatible with other results, but the accurate $k^{-5/3}$ scaling is not explained and the Kolmogorov constant is not estimated. The lack of scale invariance should produce intermittency in high-order structure functions, as observed in some but not all numerical simulations of the inverse cascade. When analogous RG methods are applied to the one-dimensional Burgers equation using an FDT-preserving dimensional continuation, equipartition is obtained instead of a cascade—in agreement with simulations.

PACS numbers: 47.27.Gs

I. INTRODUCTION

The cascade of energy to low wavenumbers in two-dimensional turbulence [1], more than other turbulence problems, is suited to the standard methods of statistical field theory and the renormalization group (RG). These methods [2], originating in quantum field theory, show that arbitrary short-distance interactions lead to long-distance behavior described by a local, renormalizable action—an effective field theory. Correlation functions computed from this action contain ultraviolet (UV) divergences that can be eliminated by redefining the parameters and fields. The divergences leave their mark, however, in the dependence on the renormalization scale and the resulting anomalous scaling laws.

The classic application of statistical field theory is to critical phenomena (second-order phase transitions) in condensed matter [2]. The infrared (IR) scale invariance of correlation functions at the transition temperature is explained by a fixed point of the RG flow. The inverse energy cascade of two-dimensional turbulence is likewise believed to be nearly scale invariant, and one might suspect that a similar fixed point is responsible. We will see, however, that no fixed point can reproduce the observed $k^{-5/3}$ energy spectrum. Rather, we will argue that the inverse cascade arises from a nontrivial RG flow and thus is not expected to be completely scale invariant.

In the study of turbulence, a deviation from scale invariance (a dependence of dimensionless physical quan-

ties on scale) is referred to as intermittency [3]. While intermittency is recognized as a property of the three-dimensional direct cascade of energy, its existence in the two-dimensional inverse cascade is unsettled. For a non-stationary inverse cascade, in which energy is not dissipated but progresses to ever-lower wavenumbers, intermittency is not observed in numerical simulations [4, 5]; a theoretical explanation has been given [6]. In this paper we deal solely with the stationary regime, where an inverse cascade requires a low-wavenumber energy sink. With few exceptions, simulations of such a cascade confirm the $k^{-5/3}$ energy spectrum initially predicted [1] on the basis of scale invariance. But one set of simulations [7] finds strong intermittency in fourth- and higher-order velocity correlations. Other simulations [8] and experiments [9], though, find no significant intermittency. The various studies differ mainly in the precise form of the dissipation terms. The evidence suggests that intermittency in the stationary inverse cascade, permitted by our theory, is at least possibly realized.

It is our restricted focus on the inverse cascade that allows us to work with a purely local field theory. The random force that stirs the fluid is correlated over a limited range and is effectively local in a long-distance description. As with the RG treatment of quantum fields and condensed matter, we expect all short-distance details to become irrelevant except as they are manifested in local, renormalizable couplings. The two-dimensional direct cascade of enstrophy to high wavenumbers [1] thus falls outside our scope. A previous RG analysis of two-dimensional turbulence [10] is formally similar to ours, but it follows three-dimensional studies by adopting the long-range force correlations necessary for a direct cas-

*Electronic address: jmayo@princeton.edu

cade; even its derivation of the inverse cascade relies on nonlocal forcing. Here we apply RG methods in the familiar domain of local field theory, which should allow a physical treatment of the inverse cascade. The explanation of the direct enstrophy cascade may rest on entirely different foundations, such as conformal invariance [11].

The work most closely aligned with our theoretical approach is due to Forster, Nelson, and Stephen (FNS) [12]. At the technical level, our contribution is to add linear friction to FNS model A in $d = 2$ and compute the RG flow to the next order of perturbation theory, two loops. The inclusion of friction, which dissipates energy at low wavenumbers, makes our theory capable in principle of describing the inverse cascade and its $k^{-5/3}$ spectrum—unlike FNS model A, which gives a k^1 spectrum corresponding to energy equipartition in $d = 2$. We also note a difference in our viewpoint from that of FNS and others [10, 13, 14] who apply RG methods to turbulence by analogy with critical phenomena. These authors seek a controlled IR-stable fixed point by starting with a logarithmically divergent field theory and then decreasing the dimension of space or the exponent of the stirring-force correlation by ϵ . This adds to the β function a negative linear term proportional to ϵ . With the usual positive one-loop term, there exists an IR-stable fixed point at a coupling that goes to zero with ϵ ; the fixed-point theory can then be expanded in ϵ instead of the original coupling. Like FNS, we work in $d = 2 - \epsilon$ to regulate UV divergences, but we ultimately take $\epsilon = 0$, so that the fixed point is trivial. Our inverse-cascade model lies not at a fixed point but in the region of large dimensionless coupling.

Naturally the use of perturbation theory is questionable for strong coupling. Our perturbative results will have direct quantitative application only to the extreme IR limit controlled by the trivial fixed point, which is of some interest in itself. Nevertheless, we will make reasonable conjectures about the theory's strong-coupling behavior that are consistent with the inverse cascade, bearing in mind the dangers of the nonperturbative regime. Besides the concern with the numerical accuracy of extrapolations, there are fundamental difficulties at strong coupling. The anomalous dimensions of operators may be large, and the relevance of terms in the action may differ from the weak-coupling case. Furthermore, at strong coupling, there is no simple relation between the couplings in different renormalization schemes, such as the Wilsonian cutoff (useful for physical interpretation) and minimal subtraction (convenient for systematic calculation). We may hope that these subtleties do not affect the main conclusions even at very strong coupling. At least we know that the theory of critical phenomena in $d = 4 - \epsilon$ is extrapolated to $\epsilon = 1$ (moderate coupling) with acceptable results.

In Sec. II we describe the basis of our theory and our method of calculation, confirming the one-loop RG flow of FNS [12]. In Sec. III we present symmetries and other properties of the theory that do not involve a dubious

extrapolation to strong coupling. In Sec. IV we compute the two-loop term of the β function. In Sec. V we relate the plausible strong-coupling behavior of the theory to the phenomenology of the inverse cascade. In Sec. VI, as a test of our methods, we consider a rather different model, the UV-stirred one-dimensional Burgers equation. A summary and discussion are presented in Sec. VII.

II. FRAMEWORK

A. Path integral for the Navier–Stokes equation

The Navier–Stokes equation for the velocity field v_j of an incompressible two-dimensional fluid is

$$\dot{v}_j + v_k \nabla_k v_j + \nabla_j P - \nu \nabla^2 v_j + \alpha v_j = f_j, \quad (1)$$

where P is the pressure divided by the density, ν is the kinematic viscosity, α is the friction coefficient, and f_j is the force per unit mass. The incompressibility condition $\nabla_i v_i = 0$ allows the velocity to be expressed as

$$v_i = \epsilon_{ij} \nabla_j \psi, \quad (2)$$

where ψ is a pseudoscalar field called the stream function and ϵ_{ij} is the alternating tensor, which in two dimensions satisfies

$$\epsilon_{ij} \epsilon_{kl} = \delta_{ik} \delta_{jl} - \delta_{il} \delta_{jk}. \quad (3)$$

Upon writing Eq. (1) in terms of ψ and applying the operator $\epsilon_{ij} \nabla_i$, we obtain [10]

$$-\nabla^2 \dot{\psi} - \epsilon_{ij} \nabla_i \nabla^2 \psi \nabla_j \psi + \nu \nabla^4 \psi - \alpha \nabla^2 \psi = \eta. \quad (4)$$

Here

$$\eta = \nabla \times \mathbf{f}, \quad (5)$$

with the notation

$$\mathbf{a} \times \mathbf{b} \equiv \epsilon_{ij} a_i b_j. \quad (6)$$

In the real three-dimensional world, Eq. (1) is a good approximation for a thin fluid film provided either (a) the boundary surface(s) and the coordinate system are rotating rapidly about a perpendicular axis or (b) the fluid is conducting and subject to a strong perpendicular magnetic field [15]. In either case, boundary-layer effects produce a linear friction parametrized by α , which has units of frequency.

For convenience, our field-theory calculations will use the method of dimensional regularization [16], based on continuation to a noninteger spatial dimension $d = 2 - \epsilon$. Because in the end we are concerned only with $d = 2$, we adopt a formal continuation of the Navier–Stokes equation that preserves its two-dimensional features. For general d , we retain the stream-function representation by choosing a “physical” two-dimensional subspace that

contains the tensor ϵ_{ij} and the external wavevectors of correlation functions. Denoting by Θ_{ij} the projector onto the physical subspace, we now have

$$\epsilon_{ij}\epsilon_{kl} = \Theta_{ik}\Theta_{jl} - \Theta_{il}\Theta_{jk}. \quad (7)$$

We take Eq. (4) as the equation of motion for ψ , with $\nabla^2 \equiv \nabla_k \nabla_k$ interpreted as the d -dimensional Laplacian. In this way we preserve (for $\nu = \alpha = \eta = 0$) the formal conservation of the energy and enstrophy,

$$E = \frac{1}{2} \int d^d x \nabla_i \psi \nabla_i \psi, \quad (8)$$

$$\Omega = \frac{1}{2} \int d^d x \nabla^2 \psi \nabla^2 \psi. \quad (9)$$

We assume that the fluid is stirred by a Gaussian random force that is uncorrelated in time [12], with

$$\begin{aligned} \langle f_i(\omega, \mathbf{k}) f_j(\omega', \mathbf{k}') \rangle &= (2\pi)^{d+1} \delta(\omega + \omega') \delta(\mathbf{k} + \mathbf{k}') \\ &\times (\delta_{ij} - k_i k_j / k^2) D(k^2), \end{aligned} \quad (10)$$

so that η is also Gaussian with

$$\langle \eta(\omega, \mathbf{k}) \eta(\omega', \mathbf{k}') \rangle = (2\pi)^{d+1} \delta(\omega + \omega') \delta(\mathbf{k} + \mathbf{k}') k^2 D(k^2). \quad (11)$$

A classical system with random forcing can be treated in the formalism of quantum field theory [17], including the path-integral representation [18, 19, 20]. Upon introduction of a pseudoscalar field p conjugate to η , correlation functions of ψ are given by the path integral

$$\langle F[\psi] \rangle \propto \int \mathcal{D}\psi \mathcal{D}p F[\psi] e^{-S}, \quad (12)$$

with the action

$$\begin{aligned} S &= \int dt d^d x \left[\frac{1}{2} (-\nabla^2 p) D(-\nabla^2) p \right. \\ &\quad \left. + ip(-\nabla^2 \dot{\psi} - \epsilon_{ij} \nabla_i \nabla^2 \psi \nabla_j \psi + \nu \nabla^4 \psi - \alpha \nabla^2 \psi) \right] \\ &= \int dt d^d x \left[\frac{1}{2} (-\nabla^2 p) D(-\nabla^2) p + i\nu p \nabla^4 \psi \right. \\ &\quad \left. - i\alpha p \nabla^2 \psi - ip \nabla^2 \dot{\psi} - i\epsilon_{ij} \nabla_i \nabla_k p \nabla_j \psi \nabla_k \psi \right], \end{aligned} \quad (13)$$

where we have integrated the $p\psi\psi$ term by parts. The Jacobian determinant from changing variables from η to ψ is an unimportant constant by virtue of causality [20].

B. Relevance of couplings

In the field theory based on the action (13), the long-distance behavior is governed by just the renormalizable terms—those with coefficients whose scaling dimensions with respect to wavenumber in $d = 2$ are zero (marginal) or positive (relevant) [2]. We assign scaling dimensions d_ψ , d_p , d_t to the fields ψ and p and to the time t by requiring that the highest-derivative quadratic terms in the action have dimensionless coefficients in $d = 2$, since

these terms control the asymptotic behavior of propagators and thus the UV convergence or divergence of diagrams. Because of the additional derivatives, the viscous term $i\nu p \nabla^4 \psi$ is clearly less relevant than the friction term $-i\alpha p \nabla^2 \psi$. In fact, it is commonly said that viscosity is irrelevant to the inverse cascade, but we now show that this cannot be taken in the technical sense. If the viscous term is ignored, then the $p \nabla^2 \psi$ and $p \nabla^2 \dot{\psi}$ terms have dimensionless coefficients only if $d_t = 0$ and $d_\psi = -d_p$. For a nontrivial theory, the $p\psi\psi$ term must be renormalizable, giving $2 \geq 4 + d_p + 2d_\psi = 4 - d_p$. With $d_p \geq 2$, there exists no local renormalizable forcing term quadratic in p .

Let us therefore retain the viscous term and recompute the scaling dimensions. The $p \nabla^4 \psi$ and $p \nabla^2 \dot{\psi}$ terms possess dimensionless coefficients only if $d_t = -2$ and $d_\psi = -d_p$. Renormalizability of the $p\psi\psi$ term now gives $4 \geq 4 + d_p + 2d_\psi = 4 - d_p$, so that $d_p \geq 0$. It remains to specify the forcing term. We assume that the external forcing is confined to a band of high wavenumbers, as in model C of FNS [12]. The effective forcing at low wavenumbers is generated by renormalization; because the interaction in Eq. (13) has two spatial derivatives acting on p , at least two derivatives must accompany each factor of p in any term so generated. The only renormalizable forcing term is then $\frac{1}{2} D_0 \nabla^2 p \nabla^2 p$, whose coefficient is dimensionless for $d_p = d_\psi = 0$. This effective forcing has $D(k^2) = D_0 k^2$, as in model A of FNS. All terms in the action are now marginal, except for the friction term, which is relevant (coefficient of dimension 2). The only other renormalizable terms that could be generated are ones containing only ψ , but these are not generated (see Sec. II C).

Next we label the fields and the time in Eq. (13) with the subscript “phys” and introduce rescaled variables to simplify the action. Tentatively seeking to set all coefficients other than forcing and friction equal to 1, we take

$$\psi_{\text{phys}} = \nu \psi, \quad p_{\text{phys}} = \nu^{-1} p, \quad t_{\text{phys}} = \nu^{-1} t. \quad (14)$$

The result is

$$\begin{aligned} S &= \int dt d^d x \left(\frac{1}{2} g^2 \nabla^2 p \nabla^2 p + ip \nabla^4 \psi \right. \\ &\quad \left. - i\nu^{-1} \alpha p \nabla^2 \psi - ip \nabla^2 \dot{\psi} - i\epsilon_{ij} \nabla_i \nabla_k p \nabla_j \psi \nabla_k \psi \right), \end{aligned} \quad (15)$$

where

$$g = D_0^{1/2} \nu^{-3/2}. \quad (16)$$

We adopt, however, a different rescaling that will be particularly convenient in Sec. III B:

$$\psi_{\text{phys}} = g\nu\psi, \quad p_{\text{phys}} = (g\nu)^{-1} p, \quad t_{\text{phys}} = (g\nu)^{-1} t. \quad (17)$$

The final form of the action is then

$$\begin{aligned} S &= \int dt d^d x \left(\frac{1}{2} g^{-1} \nabla^2 p \nabla^2 p + ig^{-1} p \nabla^4 \psi \right. \\ &\quad \left. - i\rho p \nabla^2 \psi - ip \nabla^2 \dot{\psi} - i\epsilon_{ij} \nabla_i \nabla_k p \nabla_j \psi \nabla_k \psi \right), \end{aligned} \quad (18)$$

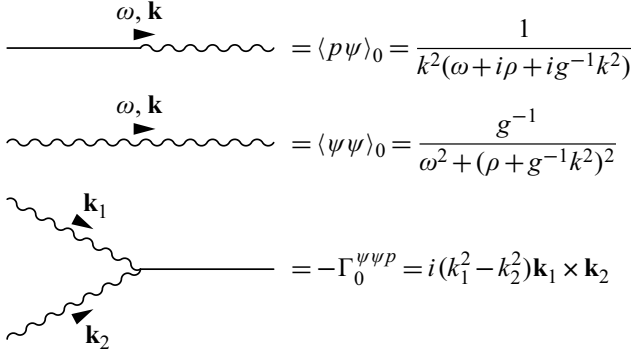


FIG. 1: Feynman rules for the action (18).

where

$$\rho = (g\nu)^{-1}\alpha = D_0^{-1/2}\nu^{1/2}\alpha. \quad (19)$$

For general $d = 2 - \epsilon$, the scaling dimensions in Eq. (18) are

$$\begin{aligned} d_\psi = d_p = -\frac{1}{2}\epsilon, \quad d_t = -2 + \frac{1}{2}\epsilon, \\ d_g = +\frac{1}{2}\epsilon, \quad d_\rho = +2 - \frac{1}{2}\epsilon. \end{aligned} \quad (20)$$

In two dimensions, g is a dimensionless coupling and ρ is analogous to a mass parameter in quantum field theory.

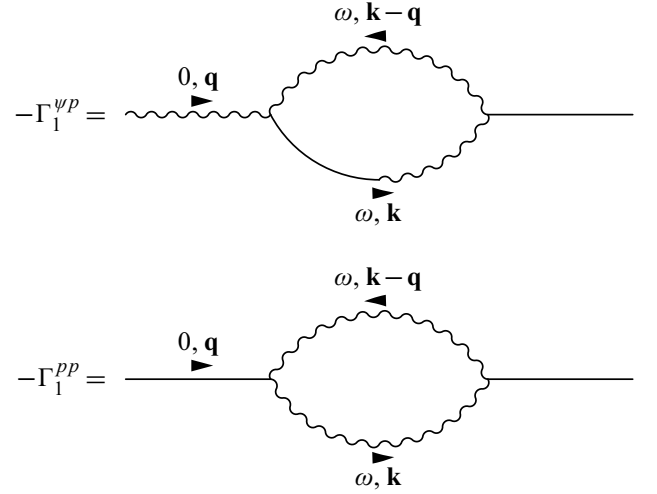
C. Feynman rules

Correlation functions can be calculated for the action (18) using Feynman diagrams whose lines carry both frequencies and wavevectors. We represent the fields ψ and p by wiggly and plain lines respectively. The ingredients of the diagrams, shown in Fig. 1, are the propagators $\langle p\psi \rangle_0$, $\langle \psi\psi \rangle_0$, obtained from the quadratic terms in the action, and the vertex factor $-\Gamma_0^{\psi\psi p}$, obtained from the cubic term. We label these quantities with the subscript 0 because they are the tree-level contributions to the exact two-point correlation functions $\langle p\psi \rangle$, $\langle \psi\psi \rangle$ and the exact three-point one-particle-irreducible (1PI) function $-\Gamma^{\psi\psi p}$.

The remaining contributions arise from diagrams containing loops. For these diagrams, we integrate over each loop frequency and wavevector according to

$$\int \frac{d\omega}{2\pi} \frac{d^d k}{(2\pi)^d}. \quad (21)$$

Because the integrand is a rational function of the frequencies, the ω integrations can easily be performed by the contour method before integrating over wavevectors. This contour integration shows that a 1PI diagram (or subdiagram) vanishes if all its external lines are ψ [20], since there is a closed loop of $\langle p\psi \rangle_0$ propagators and the integrand is an analytic function of the loop frequency in the upper half-plane.

FIG. 2: One-loop diagrams for the two-point 1PI functions $-\Gamma^{\psi p}$ and $-\Gamma^{pp}$ at zero frequency.

Unlike many field theories in a low number of spatial dimensions, ours does not contain IR divergences even for $\rho = 0$. This is because, after integration over frequencies, internal-line propagators scale as k^{-2} , but at least one further factor of the wavevector arises from each of the two vertices that a line connects. Hence the integrand does not diverge as the wavevector of any internal line goes to zero. The frequencies and wavevectors of the external lines act as an IR cutoff. For simplicity, our calculations will adopt another IR cutoff by assuming that $\rho > 0$; then 1PI diagrams are analytic at zero external frequencies and wavevectors.

D. One-loop renormalization

The coefficients of the quadratic terms in the action (with frequency χ and wavevector \mathbf{q}) are

$$\Gamma_0^{\psi p} = q^2(\chi + i\rho + ig^{-1}q^2), \quad (22)$$

$$\Gamma_0^{pp} = g^{-1}q^4. \quad (23)$$

These are corrected at one loop by the two-point 1PI diagrams in Fig. 2. Because of the external wavevectors in the vertex factors, the diagrams are $O(q^4)$, and so we can set $\chi = 0$. We now demonstrate the computation of the $-\Gamma_1^{\psi p}$ diagram, to show the basic methods to be used for two-loop diagrams in Sec. IV.

The frequency integral of the propagators is

$$\begin{aligned} I &\equiv \int_{-\infty}^{\infty} \frac{d\omega}{2\pi} [g^{-1}k^{-2}(\omega + i\rho + ig^{-1}k^2)^{-1} \\ &\quad \times (\omega + i\rho + ig^{-1}|\mathbf{k} - \mathbf{q}|^2)^{-1}(\omega - i\rho - ig^{-1}|\mathbf{k} - \mathbf{q}|^2)^{-1}] \\ &= \frac{-ig/4k^2}{(g\rho + k^2 - \mathbf{k} \cdot \mathbf{q} + \frac{1}{2}q^2)(g\rho + k^2 - 2\mathbf{k} \cdot \mathbf{q} + q^2)}, \end{aligned} \quad (24)$$

obtained conveniently by closing the contour in the upper half-plane and picking up one pole. We next multiply by the vertex factors and expand to $O(q^4)$:

$$\begin{aligned} & i(k^2 - 2\mathbf{k} \cdot \mathbf{q})(\mathbf{k} \times \mathbf{q}) i(2\mathbf{k} \cdot \mathbf{q} - q^2)(\mathbf{k} \times \mathbf{q}) I \\ &= (k^2 - 2\mathbf{k} \cdot \mathbf{q})(q^2 - 2\mathbf{k} \cdot \mathbf{q})[k_{\parallel}^2 q^2 - (\mathbf{k} \cdot \mathbf{q})^2] I \\ &\rightarrow \frac{6ig(\mathbf{k} \cdot \mathbf{q})^2[k_{\parallel}^2 q^2 - (\mathbf{k} \cdot \mathbf{q})^2]}{4(g\rho + k^2)^3} \\ &\quad - \frac{ig[k^2 q^2 + 4(\mathbf{k} \cdot \mathbf{q})^2][k_{\parallel}^2 q^2 - (\mathbf{k} \cdot \mathbf{q})^2]}{4k^2(g\rho + k^2)^2}, \end{aligned} \quad (25)$$

where $k_{\parallel}^2 \equiv \Theta_{ij} k_i k_j$ is the squared projection of \mathbf{k} onto the physical subspace and we infer from Eq. (7) that

$$(\mathbf{k} \times \mathbf{q})^2 = k_{\parallel}^2 q^2 - (\mathbf{k} \cdot \mathbf{q})^2. \quad (26)$$

We omit $O(q^3)$ terms in Eq. (25) because they will now disappear when we average over directions of \mathbf{k} .

With the d -dimensional isotropization formulas

$$k_i k_j \rightarrow k^2 \frac{\delta_{ij}}{d}, \quad k_i k_j k_k k_l \rightarrow k^4 \frac{\delta_{ij} \delta_{kl} + \delta_{ik} \delta_{jl} + \delta_{il} \delta_{jk}}{d(d+2)}, \quad (27)$$

which imply

$$\begin{aligned} k_{\parallel}^2 &\rightarrow \frac{2k^2}{d}, & (\mathbf{k} \cdot \mathbf{q})^2 &\rightarrow \frac{k^2 q^2}{d}, \\ (\mathbf{k} \cdot \mathbf{q})^2 k_{\parallel}^2 &\rightarrow \frac{4k^4 q^2}{d(d+2)}, & (\mathbf{k} \cdot \mathbf{q})^4 &\rightarrow \frac{3k^4 q^4}{d(d+2)}, \end{aligned} \quad (28)$$

the value of the diagram to $O(q^4)$ becomes

$$\begin{aligned} -\Gamma_1^{\psi p} &= -igq^4 \\ &\times \int_0^\infty \frac{dk}{(2\pi)^d} \frac{2\pi^{d/2} k^{d-1}}{\Gamma(\frac{1}{2}d)} k^2 \frac{(6+d)g\rho + dk^2}{4d(d+2)(g\rho + k^2)^3} \\ &= -igq^4 \frac{6-d}{(2+d)2^{4+d}\Gamma(\frac{1}{2}d)\sin(\frac{1}{2}\pi d)} \left(\frac{\pi}{g\rho}\right)^{1-d/2}. \end{aligned} \quad (29)$$

For $d = 2 - \epsilon$ with $\epsilon \rightarrow 0$, we find

$$+\Gamma_1^{\psi p} = igq^4 \left(\frac{1}{32\pi\epsilon} - \frac{\ln(g\rho/4\pi) + \gamma_E - 1}{64\pi} + O(\epsilon) \right), \quad (30)$$

where γ_E is the Euler constant. The result for the other one-loop diagram (taking into account the symmetry factor) is very similar:

$$+\Gamma_1^{pp} = gq^4 \left(\frac{1}{32\pi\epsilon} - \frac{\ln(g\rho/4\pi) + \gamma_E}{64\pi} + O(\epsilon) \right). \quad (31)$$

We have carefully obtained the $O(\epsilon^0)$ terms, which will be important in Sec. IV.

The method of minimal subtraction [21] expresses the bare couplings g and ρ , of respective dimensions $\frac{1}{2}\epsilon$ and

$2 - \frac{1}{2}\epsilon$, in terms of a renormalization scale μ (dimension 1) and dimensionless renormalized couplings \bar{g} and $\bar{\rho}$ as

$$g = \mu^{\epsilon/2} [\bar{g} + \bar{g}^3 a_1 \epsilon^{-1} + O(\bar{g}^5)], \quad (32)$$

$$\rho = \mu^{2-\epsilon/2} \bar{\rho}, \quad (33)$$

where the corrections (called counterterms) involve only negative powers of ϵ . The coefficient of the $O(\bar{g}^3)$ counterterm, and the absence of any counterterms for $\bar{\rho}$, are obtained by requiring that $\Gamma^{\psi p}$ and Γ^{pp} to $O(q^4)$ be finite at $\epsilon = 0$ when expressed in terms of \bar{g} and $\bar{\rho}$:

$$\begin{aligned} \Gamma^{\psi p} &= q^2(\chi + i\rho) \\ &\quad + iq^4 \left[g^{-1} + g \left(\frac{1}{32\pi\epsilon} + O(\epsilon^0) \right) + O(g^3) \right] \\ &= q^2(\chi + i\mu^{2-\epsilon/2} \bar{\rho}) \\ &\quad + iq^4 \mu^{-\epsilon/2} \\ &\quad \times \left[\bar{g}^{-1} + \bar{g} \left(\frac{1}{32\pi\epsilon} - \frac{a_1}{\epsilon} + O(\epsilon^0) \right) + O(\bar{g}^3) \right], \end{aligned} \quad (34)$$

$$\begin{aligned} \Gamma^{pp} &= q^4 \mu^{-\epsilon/2} \\ &\quad \times \left[\bar{g}^{-1} + \bar{g} \left(\frac{1}{32\pi\epsilon} - \frac{a_1}{\epsilon} + O(\epsilon^0) \right) + O(\bar{g}^3) \right]. \end{aligned} \quad (35)$$

Hence

$$a_1 = \frac{1}{32\pi}, \quad (36)$$

and no counterterms of any order are needed for $\bar{\rho}$ because the q^2 term of $\Gamma^{\psi p}$ is not renormalized.

As for the three-point 1PI function $-\Gamma^{\psi\psi p}$, we will see in Sec. III A that it is related by Galilean invariance to the $q^2\chi$ term of $\Gamma^{\psi p}$. Because the latter term is not renormalized, we have

$$-\Gamma^{\psi\psi p} = -\Gamma_0^{\psi\psi p} = i(k_1^2 - k_2^2)\mathbf{k}_1 \times \mathbf{k}_2, \quad (37)$$

up to irrelevant terms with more factors of wavevector. We have thus rendered the theory finite at one loop by renormalizing only the coupling \bar{g} , without the need for counterterms to rescale the fields ψ and p or the time t . Crucial for this was the equality of the $1/32\pi\epsilon$ terms in Eqs. (30) and (31). We conclude that the anomalous dimensions are zero at one loop, and in Sec. III B we will show that in minimal subtraction they are exactly zero,

$$\gamma_\psi = \gamma_p = \gamma_t = 0. \quad (38)$$

In a different renormalization scheme, or with a different definition of the fields and the time such as Eq. (14), the anomalous dimensions would not vanish identically, but at any RG fixed point their values are universal [2] and so they would be zero there.

The β functions for the dimensionless couplings are determined by the RG invariance of the bare couplings,

$$\left(\mu \frac{\partial}{\partial \mu} + \beta(\bar{g}) \frac{\partial}{\partial \bar{g}} + \beta(\bar{\rho}) \frac{\partial}{\partial \bar{\rho}} \right) \left\{ \frac{g}{\rho} \right\} = 0. \quad (39)$$

We obtain

$$\beta(\bar{g}) = -\frac{1}{2}\epsilon\bar{g} + \frac{\bar{g}^3}{32\pi} + O(\bar{g}^5), \quad (40)$$

$$\beta(\bar{\rho}) = (-2 + \frac{1}{2}\epsilon)\bar{\rho}. \quad (41)$$

The force correlation adopted by FNS [12] differs from Eq. (10) by a factor of 2, and consequently the dimensionless coupling of FNS is $\bar{\lambda} = 2^{-1/2}\bar{g}$. Thus we have confirmed the FNS result

$$\beta(\bar{\lambda}) = -\frac{1}{2}\epsilon\bar{\lambda} + \frac{\bar{\lambda}^3}{16\pi} + O(\bar{\lambda}^5). \quad (42)$$

III. GENERAL PROPERTIES

A. Galilean invariance

In two dimensions, the equation of motion (4) and thus the action (18) have the important physical property of invariance under a Galilean transformation to a reference frame moving with constant velocity \mathbf{u} [12, 13, 20]. This property depends on the assumption that the stirring force is uncorrelated in time, since otherwise there would exist a link between a point in space at one time and a “corresponding” point in space at a different time. Specifically, the action (18) is invariant under the transformation

$$\begin{aligned} \psi(t, \mathbf{x}) &\rightarrow \psi(t, \mathbf{x} + \mathbf{u}t) + \epsilon_{ij}x_i u_j, \\ p(t, \mathbf{x}) &\rightarrow p(t, \mathbf{x} + \mathbf{u}t), \end{aligned} \quad (43)$$

which induces the familiar transformation of the velocity,

$$\mathbf{v}(t, \mathbf{x}) \rightarrow \mathbf{v}(t, \mathbf{x} + \mathbf{u}t) - \mathbf{u}. \quad (44)$$

The original Navier–Stokes equation (1) is not Galilean invariant because of the friction term, which introduces a preferred state of rest; but the differentiation in deriving the stream-function equation (4) eliminates the constant shift in \mathbf{v} [10].

We would not expect Galilean invariance in $d = 2$ to be preserved by our renormalization method unless the theory remains Galilean invariant when dimensionally regulated. We now show that our formal stream-function representation in arbitrary d is invariant under the transformation (43), provided that \mathbf{u} lies in the physical subspace. For convenience we use the infinitesimal form

$$\delta\psi = tu_i \nabla_i \psi + \epsilon_{ij}x_i u_j, \quad \delta p = tu_i \nabla_i p. \quad (45)$$

In the corresponding variation of the action (18), terms proportional to t vanish automatically because they correspond to a simple spatial translation. The interesting terms are those where the t is differentiated ($-ip\nabla^2\psi$) and where ψ is varied by $\epsilon_{ij}x_i u_j$. Neither of these affects

the forcing, viscous, or friction terms, which contain ψ only as $\nabla^2\psi$ and are trivially invariant. We are left with

$$\begin{aligned} \delta S = - \int dt d^d x & (ipu_i \nabla_i \nabla^2 \psi + i\epsilon_{ij} \nabla_i \nabla_k p \epsilon_{jl} u_l \nabla_k \psi \\ & + i\epsilon_{ij} \nabla_i \nabla_k p \nabla_j \psi \epsilon_{kl} u_l). \end{aligned} \quad (46)$$

Upon integration by parts and use of $\Theta_{il}u_l = u_i$, the first two terms cancel and the third vanishes.

In Fourier space, the transformation (45) becomes

$$\begin{aligned} \delta\psi(\omega, \mathbf{k}) &= \mathbf{u} \cdot \mathbf{k} \frac{\partial}{\partial\omega} \psi(\omega, \mathbf{k}) - i(2\pi)^{d+1} \delta(\omega) \mathbf{u} \times \nabla \delta(\mathbf{k}), \\ \delta p(\omega, \mathbf{k}) &= \mathbf{u} \cdot \mathbf{k} \frac{\partial}{\partial\omega} p(\omega, \mathbf{k}). \end{aligned} \quad (47)$$

The action is Galilean invariant by virtue of the relation

$$\mathbf{u} \cdot \mathbf{k} \frac{\partial}{\partial\omega} \Gamma_0^{\psi p}(\omega, \mathbf{k}) = i\mathbf{u} \times \nabla' \Gamma_0^{\psi\psi p}(\omega, \mathbf{k}; 0, \mathbf{k}')|_{\mathbf{k}'=0}; \quad (48)$$

both sides equal $\mathbf{u} \cdot \mathbf{k} k^2$. The same relation must then hold between the exact 1PI functions: The coefficient of $k^2\omega$ in $\Gamma^{\psi p}$ equals the coefficient of $-i(k_1^2 - k_2^2)\mathbf{k}_1 \times \mathbf{k}_2$ in $\Gamma^{\psi\psi p}$. Since the former is not renormalized, neither is the latter.

B. Fluctuation-dissipation theorem

For zero friction ($\rho = 0$), the action (18) is equivalent to model A of FNS [12], who note that it obeys detailed balance and thus is subject to a classical fluctuation-dissipation theorem (FDT) [22]. A complicated diagrammatic argument demonstrates that the FDT is preserved to all orders of renormalization [22]. Here we reach this conclusion by obtaining the FDT from an exact symmetry of the action in arbitrary d . Under the formal discrete transformation

$$p \rightarrow p - 2i\psi, \quad (49)$$

the action with $\rho = 0$ changes only by reversing the sign of the viscous term. The change in the interaction term vanishes upon integration by parts, just as in deriving conservation of energy. To restore the sign of the viscous term, we further perform a complete time reversal,

$$t \rightarrow -t, \quad \psi \rightarrow -\psi, \quad (50)$$

which naturally reverses the sign of the dissipation. The net effect is the transformation

$$p(t) \rightarrow p(-t) + 2i\psi(-t), \quad \psi(t) \rightarrow -\psi(-t), \quad (51)$$

a generalized time reversal that is its own inverse and leaves the action invariant.

The FDT is derived from this symmetry by expressing the invariance of $\langle p\psi \rangle$:

$$\langle p\psi \rangle = -\langle \psi p \rangle - 2i\langle \psi\psi \rangle. \quad (52)$$

By invariance under time translations and spatial rotations, negating the times in a two-point correlation function is equivalent to interchanging the points. As a first application of the FDT, we make use of the theorem that the equal-time correlation function $\langle p\psi \rangle_+ = \langle \psi p \rangle_+$ is exact at tree level [20]. Thus, for $\rho = 0$, the exact equal-time stream-function correlation is

$$\begin{aligned} \langle \psi\psi \rangle_+ &= \frac{1}{2}i(\langle p\psi \rangle_+ + \langle \psi p \rangle_+) \\ &= \frac{1}{2}i \int_{-\infty}^{\infty} \frac{d\omega}{2\pi} (\langle p\psi \rangle_0 + \langle \psi p \rangle_0) \\ &= \frac{1}{2}i \int_{-\infty}^{\infty} \frac{d\omega}{2\pi} \frac{-2ig^{-1}}{\omega^2 + g^{-2}k^4} = \frac{1}{2k^2}. \end{aligned} \quad (53)$$

The energy spectrum, in the units implied by Eq. (17), is then

$$E(k) = \frac{\pi k}{(2\pi)^2} k^2 \langle \psi\psi \rangle_+ = \frac{k}{8\pi}. \quad (54)$$

This is an equipartition spectrum, in agreement with FNS model A [12].

For $\rho = 0$, the FDT (52) also implies that, if $\langle p\psi \rangle$ and thus $\langle \psi p \rangle$ are made finite by renormalizing \bar{g} , then $\langle \psi\psi \rangle$ is likewise finite, without the need for field or time rescalings. As we have seen, the three-point 1PI function is automatically finite. Hence the anomalous dimensions vanish exactly for $\rho = 0$. But in minimal subtraction, the counterterms for rescalings and for dimensionless couplings are independent of the mass parameter [21]. We conclude that in minimal subtraction, even with friction,

$$\gamma_\psi = \gamma_p = \gamma_t = 0, \quad (55)$$

and $\beta(\bar{g})$ depends only on \bar{g} . Indeed, we have seen these statements verified to one loop in Sec. II D.

C. Renormalization-group flows

We have shown that the anomalous dimensions vanish, and that the renormalized couplings in exactly two dimensions obey

$$\mu \frac{d\bar{g}}{d\mu} \equiv \beta(\bar{g}) = \frac{\bar{g}^3}{32\pi} + O(\bar{g}^5), \quad (56)$$

$$\bar{\rho} = \mu^{-2}\rho. \quad (57)$$

Thus $\bar{\rho}$ is very simply related to μ and can be used to parametrize it. In the RG flow to low wavenumbers, $\bar{\rho}$ steadily increases as friction becomes more important. Meanwhile, \bar{g} flows in its own characteristic way regardless of the value of $\bar{\rho}$; the most we can say is that once \bar{g} becomes small, it decreases further and further, approaching zero in the IR limit. The solution of Eq. (56) in this limit is

$$\bar{g}(\mu) = \sqrt{\frac{16\pi}{\ln(k_g/\mu)}} \quad (\mu \ll k_g), \quad (58)$$

where k_g is the scale at which \bar{g} becomes large.

In the IR limit, we expect good accuracy from perturbative results such as the tree-level expression for the energy spectrum,

$$E(k) = \frac{\pi k}{(2\pi)^2} k^2 \langle \psi\psi \rangle_+ = \frac{k^3}{8\pi(g\rho + k^2)}. \quad (59)$$

We might suppose that the true asymptotic behavior is given by replacing g with the renormalized coupling $\bar{g}(k)$. This would follow from RG theory if the loop corrections to Eq. (59) contained $\ln(k^2)$. But with $g\rho$ providing an IR cutoff, the diagrams are regular as $k \rightarrow 0$ and instead contain $\ln(g\rho)$. Hence, for the purposes of correlation functions, the RG flow effectively halts for wavenumbers below the “mass” $\sqrt{g\rho}$. If m is the suitably renormalized value of this mass, then as $k \rightarrow 0$ we expect that

$$E(k) = \frac{k^3}{8\pi\rho\bar{g}(m)}. \quad (60)$$

On the other hand, in the bare tree-level result (59), g can be interpreted as a coupling renormalized at a very high wavenumber (the forcing scale or UV cutoff). With $\beta(\bar{g}) > 0$, we have $\bar{g}(m) < g$, and so the RG result (60) gives a greater $E(k)$ at low k . Whereas the bare tree-level calculation ignores all interactions between scales, the effect of renormalization is to place more energy and dissipation at low k (and therefore less at high k), consistent with the inverse cascade.

From Eq. (57), any RG fixed point $(\bar{g}_*, \bar{\rho}_*)$ must have $\bar{\rho}_* = 0$. Not only do the anomalous dimensions vanish at any fixed point, but for $\bar{\rho} = 0$ we have the exact equipartition spectrum $E(k) \propto k^1$, whether \bar{g} is at a fixed point or not. It is clear that, despite the suggestive evidence of scale invariance of the inverse cascade, an RG fixed point in our framework cannot be the explanation for the observed $k^{-5/3}$ spectrum. Nevertheless our theory contains all the essential ingredients that have produced the stationary inverse cascade experimentally and numerically. A natural explanation is that the $k^{-5/3}$ spectrum arises from the nonperturbative behavior of correlation functions at $\bar{\rho} > 0$ and at large values of \bar{g} that flow rapidly with scale. Although it is far from obvious how such an RG flow can produce approximate scale invariance with an effective anomalous dimension, we are motivated to seek hints about the theory’s strong-coupling behavior. The first step, which can be useful for more mundane purposes as well, is to extend the renormalization to the next order of perturbation theory.

IV. TWO-LOOP RENORMALIZATION

A. Renormalization prescription and diagrams

Calculating $\beta(\bar{g})$ consistently to two loops requires a precise specification of the renormalization scheme. Remarkably, though, as long as $\beta(\bar{g})$ depends only on \bar{g} , the

β function to two loops (but no further) is independent of the particular scheme chosen [2]. As in Sec. IID, we take $\rho > 0$, compute two-point 1PI diagrams to $O(q^4)$ expanded about $\epsilon = 0$, and renormalize by minimal subtraction. The two-loop expression for the bare coupling in terms of the renormalized coupling is

$$g = \mu^{\epsilon/2} [\bar{g} + \bar{g}^3 a_1 \epsilon^{-1} + \bar{g}^5 (a_2 \epsilon^{-2} + a_2' \epsilon^{-1}) + O(\bar{g}^7)]. \quad (61)$$

With zero anomalous dimensions, $\beta(\bar{g})$ is the only RG function to be determined and we need only compute a single 1PI function to two loops. Below we will choose $-\Gamma^{pp}$ because its two-loop diagrams are technically simpler than those of $-\Gamma^{\psi p}$.

We have seen that $g\rho$, which has dimension 2 independent of ϵ , acts as the IR cutoff for wavevector integrals. By dimensional analysis, Γ^{pp} to $O(q^4)$ has the form

$$\begin{aligned} \Gamma^{pp} &= q^4 \left[g^{-1} + g(g\rho)^{-\epsilon/2} \left(\frac{b_1}{\epsilon} + b_1' + O(\epsilon) \right) \right. \\ &\quad \left. + g^3 (g\rho)^{-\epsilon} \left(\frac{b_2}{\epsilon^2} + \frac{b_2'}{\epsilon} + O(\epsilon^0) \right) + O(g^5) \right] \\ &= q^4 \left[g^{-1} + g \left(\frac{b_1}{\epsilon} + b_1' - \frac{1}{2} b_1 \ln(g\rho) + O(\epsilon) \right) \right. \\ &\quad \left. + g^3 \left(\frac{b_2}{\epsilon^2} + \frac{b_2' - b_2 \ln(g\rho)}{\epsilon} + O(\epsilon^0) \right) + O(g^5) \right]. \end{aligned} \quad (62)$$

To simplify the two-loop calculations we formally set $\rho = g^{-1}$ and restore the $\ln(g\rho)$ terms at the end.

Multiloop diagrams can be characterized by their overall UV divergence (as all loop frequencies and wavenumbers go to infinity together) and their subdivergences (as a subset of loop frequencies and wavenumbers go to infinity while the rest remain finite). Overlapping divergences occur when two or more divergent subdiagrams share a propagator; this is a definite complication in evaluating a diagram, though not insurmountable [2]. Some two-loop diagrams for the 1PI function $-\Gamma^{\psi p}$ contain overlapping divergences, so we choose to calculate the diagrams for $-\Gamma^{pp}$, which fortunately do not (Fig. 3). A three-point 1PI subdiagram is divergent only if its external lines are $\psi\psi p$, two wiggly and one plain; Galilean invariance does not eliminate this subdivergence when we treat each two-loop diagram separately, because the finiteness of $-\Gamma_1^{\psi\psi p}$ results from a sum over distinct one-loop diagrams. In Fig. 3 we have omitted one conceivable diagram containing the 1PI subdiagram $-\Gamma_1^{\psi\psi}$, which vanishes as noted in Sec. IIC.

Previous two-loop calculations of similar complexity have been made for different problems using diagrams of the same topology: the Burgers–Kardar–Parisi–Zhang equation for interface growth [23] and the Navier–Stokes equation in more than two physical dimensions, where there are fewer divergences [24].

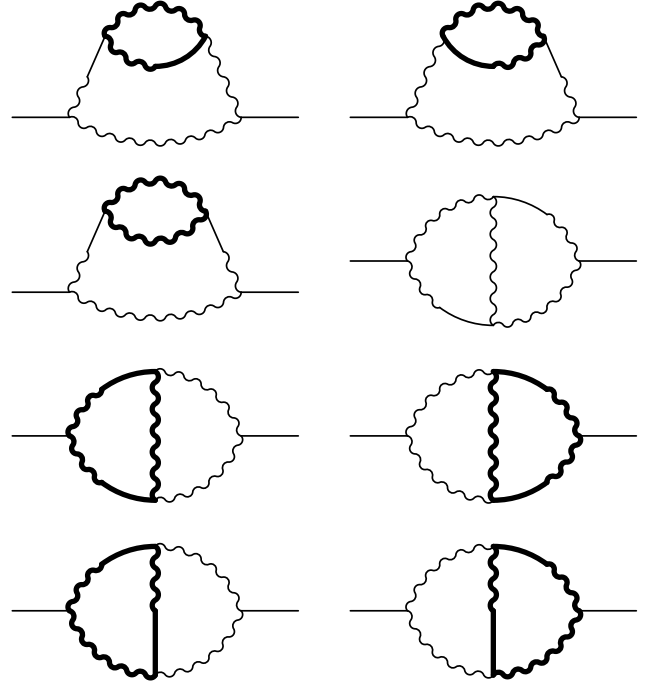


FIG. 3: Nonvanishing two-loop diagrams for the two-point 1PI function $-\Gamma^{pp}$. Along with the overall divergence, each diagram has at most one divergent subdiagram (bold lines).

B. Analytic calculations

We have programmed MATHEMATICA [25] to automate the steps in evaluating each two-loop diagram. The loop frequencies are integrated one after the other by adding the residues of all poles in the upper half-plane. The resulting integrand, containing the external wavevector \mathbf{q} and the loop wavevectors $\mathbf{k}_{1,2}$, is expanded to $O(q^4)$ and averaged over directions of \mathbf{q} in the physical subspace. The numerator of the integrand is now rife with the projector Θ_{ij} , both from averaging $q_i q_j$ and from applying Eq. (7) to cross products. To eliminate Θ_{ij} , we average the integrand over orientations of the physical subspace within d -dimensional space: We introduce an orthonormal physical basis, write $\Theta_{ij} = \hat{a}_i \hat{a}_j + \hat{b}_i \hat{b}_j$, average over directions of $\hat{\mathbf{a}}$ in the $d-1$ dimensions perpendicular to $\hat{\mathbf{b}}$, and then average over directions of $\hat{\mathbf{b}}$ in d -dimensional space. The result is a function of k_1^2 , k_2^2 , and $\mathbf{k}_1 \cdot \mathbf{k}_2$ to be integrated over $d^d k_1 d^d k_2$.

Because we need only the divergent parts of the two-loop diagrams as indicated in Eq. (62), we eliminate numerator terms that produce neither an overall divergence nor a subdivergence by power counting. We seek to integrate first over the loop wavevector (say \mathbf{k}_1) associated with the subdivergence (if any). To simplify the denominator, Feynman parameters [2] are introduced, and \mathbf{k}_1 is translated by a multiple of \mathbf{k}_2 . After the numerator is isotropized, the \mathbf{k}_1 integration is done analytically; there remains an integral over Feynman parameters and over

the magnitude k_2 . From Eq. (62), the integrand (excluding $g^3 q^4$) has dimension $-1 - 2\epsilon$. The part that behaves like $k_2^{-1-2\epsilon}$ as $k_2 \rightarrow \infty$ is subtracted and separately integrated over k_2 , producing another ϵ^{-1} factor; all the ϵ^{-2} terms arise here and are found analytically, but the ϵ^{-1} terms involve intractable Feynman-parameter integrals. Meanwhile, the remaining subtracted integral converges at $k_2 = \infty$ but contains analytically integrable ϵ^{-1} poles from the \mathbf{k}_1 integration.

Adding the divergent parts of the eight diagrams gives

$$\Gamma_2^{pp} = g^3 q^4 \left(-\frac{1}{2048\pi^2\epsilon^2} + \frac{-2\ln(4\pi) + 2\gamma_E + 5 + X}{4096\pi^2\epsilon} + O(\epsilon^0) \right). \quad (63)$$

Here X is a sum of Feynman-parameter integrals of complicated rational functions with integer coefficients; thus we expect that X may be a rational number. Though we are unable to calculate X analytically, Eq. (63) already displays some important features: If the ϵ^{-2} term were different, the renormalization performed below would become inconsistent [21]; and if the coefficients of γ_E and $\ln(4\pi)$ were different, these constants would (contrary to expectation) appear in the two-loop β function.

C. Numerical calculations

We have evaluated X numerically by multidimensional Monte Carlo integration, using the technique of importance sampling [26] to select more points in the “corners” of Feynman-parameter space (with one parameter near 1 and the others near 0). This technique improves the statistics because the integrands tend to diverge in these corners (but slowly enough that the integrals converge). We treat the integrals that make up X separately, since they vary in complexity and in number of Feynman parameters. To optimize the precision of the result for X in a given computation time T , we reason as follows. The contribution to X from diagram i , evaluated with n_i sample points, is obtained with a precision $s_i = \sigma_i n_i^{-1/2}$ in a time $t_i = \tau_i n_i$, where σ_i and τ_i are characteristics of the integrand and the computer. Constrained optimization shows that we achieve the best overall precision

$$S^2 = \sum_i s_i^2 \quad (64)$$

in the time

$$T = \sum_i t_i \quad (65)$$

by choosing

$$n_i = \frac{T\sigma_i}{\tau_i^{1/2} \sum_j \sigma_j \tau_j^{1/2}}. \quad (66)$$

Short runs are made to estimate σ_i and τ_i , and then the high-precision integrations are performed with this plan. Our computations for a total of 3.6×10^8 sample points yield

$$X = -3.995 \pm 0.005, \quad (67)$$

strongly suggesting that the exact value is

$$X = -4. \quad (68)$$

With the one-loop result (31) and the two-loop result (63), we have

$$\Gamma^{pp} = q^4 \left[g^{-1} + g \left(\frac{1}{32\pi\epsilon} - \frac{\ln(g\rho/4\pi) + \gamma_E}{64\pi} + O(\epsilon) \right) + g^3 \left(-\frac{1}{2048\pi^2\epsilon^2} + \frac{2\ln(g\rho/4\pi) + 2\gamma_E + 1}{4096\pi^2\epsilon} + O(\epsilon^0) \right) + O(g^5) \right]. \quad (69)$$

By substituting Eq. (61) and requiring a finite expression at $\epsilon = 0$, we determine

$$a_1 = \frac{1}{32\pi}, \quad a_2 = \frac{3}{2048\pi^2}, \quad a'_2 = -\frac{1}{4096\pi^2}. \quad (70)$$

The RG invariance of the bare coupling g finally gives

$$\beta(\bar{g}) = -\frac{1}{2}\epsilon\bar{g} + \frac{\bar{g}^3}{32\pi} - \frac{\bar{g}^5}{2048\pi^2} + O(\bar{g}^7). \quad (71)$$

This is reminiscent of the β function in four-dimensional ϕ^4 theory, where similarly the one-loop term is positive and the two-loop term is negative [2]. A positive β function that grows too quickly (faster than linearly) at large coupling raises the question of whether the coupling becomes infinite at a large but finite renormalization scale. In our theory this would suggest an absolute limit on the extent of the scaling range for any inverse cascade. To avoid such a fate, the expansion of the β function must contain many negative terms to slow its initial superlinear growth. It is pleasing to find such a term already at two loops.

V. INVERSE-CASCADE RANGE

A. Inverse-cascade phenomenology

The initial prediction of the two-dimensional inverse energy cascade [1] assumed zero friction and small but nonzero viscosity. Kinetic energy, continually injected at high wavenumbers, is expected to cascade down through a quasisteady inertial range extending to lower and lower wavenumbers as time passes. Within this range, the assumption of scale invariance implies the energy spectrum

$$E(k) = C \mathcal{E}^{2/3} k^{-5/3}, \quad (72)$$

where C is the two-dimensional Kolmogorov constant and \mathcal{E} is the rate of energy injection per unit mass. Numerical simulations with zero friction [4, 5, 27] confirm this spectrum until the cascade approaches the minimum wavenumber associated with a finite system. Both non-stationary behavior and finite-size effects, however, lie outside our theoretical framework, which treats a fluid of infinite size that has been stirred for an infinite time. In the absence of friction, such a fluid has an equipartition spectrum as shown in Sec. IIIB.

When friction is introduced, it is natural to expect a mirror image of the viscous energy dissipation at high wavenumbers in the three-dimensional direct cascade: A stationary inverse cascade should develop, with dissipation by friction at low wavenumbers $k \sim k_{\text{fr}}$ and with the spectrum (72) at wavenumbers $k \gg k_{\text{fr}}$ where dissipation is unimportant. Dimensional analysis gives

$$k_{\text{fr}} = \mathcal{E}^{-1/2} \alpha^{3/2}, \quad (73)$$

where α is the friction coefficient [8, 28]. Several numerical simulations [5, 8] and laboratory experiments [9, 29] confirm this picture. Other numerical studies obtain similar results but are more difficult to relate to our framework, since they modify the friction term by removing derivatives [7] or by applying friction only below a cutoff wavenumber [30]. We are less concerned about the common practice of adding derivatives to the viscous term (hyperviscosity), because such a modified term is irrelevant and the RG flow should introduce a normal viscous term to replace it. But friction modified with inverse derivatives (hypofriction) is certainly relevant and is believed to alter the dynamics of the inverse cascade [5, 8]. In an extreme case, hypofriction with eight inverse Laplacians destroys the $k^{-5/3}$ spectrum [31]. Hypofriction is intended to confine dissipation explicitly to low wavenumbers; ordinary linear friction accomplishes the same thing more gently, but makes it difficult in practice to achieve an inertial range [28]. We have used linear friction because it is physically realistic and leads to a local field theory.

For convenience in relating the observed inverse cascade to our field theory with the action (18), we adopt units of time in which

$$g\nu \equiv D_0^{1/2} \nu^{-1/2} = 1, \quad (74)$$

so that the rescalings in Eq. (17) are trivial. Then the kinematic viscosity is

$$\nu = g^{-1}, \quad (75)$$

the friction coefficient is

$$\alpha = \rho, \quad (76)$$

and the force correlation is

$$D(k^2) = g^{-1} k^2. \quad (77)$$

In contrast to the formal methods of dimensional regularization and minimal subtraction, a simple UV cutoff renders our theory finite in a physically meaningful way while still preserving the symmetries noted in Sec. III. A cutoff would have been inconvenient for the two-loop calculations of Sec. IV, but it is appropriate for understanding experimental and numerical results on the inverse cascade. The local, renormalizable action (18) applies only with a UV cutoff Λ below the wavenumbers of the external forcing [12]. A corresponding renormalization prescription is obtained by staying in exactly two spatial dimensions and writing the coupling g in Eq. (18) as a cutoff-dependent quantity $\hat{g}(\Lambda)$, such that the long-distance behavior is independent of Λ . No cutoff dependence is needed for ρ , because the friction term is not renormalized, as we saw in Sec. IID.

Special properties of minimal subtraction allowed us to conclude (Sec. IIIB) that in that scheme the anomalous dimensions vanish and $\beta(\bar{g})$ depends only on \bar{g} . We may expect that in the cutoff scheme these statements remain approximately true, at least for small values of the dimensionless friction parameter $\Lambda^{-2}\rho$. Because the β function is scheme independent through two loops [2], we have

$$\Lambda \frac{d\hat{g}}{d\Lambda} \equiv \beta(\hat{g}) = \frac{\hat{g}^3}{32\pi} - \frac{\hat{g}^5}{2048\pi^2} + O(\hat{g}^7). \quad (78)$$

This result is directly useful for weak coupling, but can only hint at the possible strong-coupling behavior. We will now show that a specific strong-coupling form of the β function is required for a fully developed inverse cascade, and that it can be naturally interpolated with the two-loop result (78).

B. Strong-coupling behavior

The key condition for the ideal inverse cascade is that the dissipation of energy is dominated by friction and is almost totally confined to low wavenumbers. This means that the dissipation rate

$$\mathcal{E} = 2\rho \int_0^\Lambda dk E(k) = 2\rho \int_0^\Lambda dk \frac{\pi k}{(2\pi)^2} k^2 \langle \psi \psi \rangle = \quad (79)$$

should be independent of the UV cutoff Λ , because a change in Λ produces neither a renormalization of ρ nor a rescaling of ψ . Under stationary conditions, \mathcal{E} equals the rate of energy injection, given by [14]

$$\mathcal{E} = \int_0^\Lambda dk \frac{\pi k}{(2\pi)^2} D(k^2) = \frac{\Lambda^4}{16\pi \hat{g}(\Lambda)}, \quad (80)$$

in terms of the force correlation (77). For \mathcal{E} to be independent of Λ , we must have the strong-coupling behavior

$$\hat{g}(\Lambda) \simeq \text{const} \times \Lambda^4, \quad (81)$$

corresponding to the asymptotically linear β function

$$\beta(\hat{g}) \simeq 4\hat{g} \quad (\hat{g} \rightarrow \infty). \quad (82)$$

We now attempt to connect this form with the two-loop β function (78).

Perturbative expansions such as Eq. (78) are usually divergent, but a Borel transformation is expected to produce a finite radius of convergence about zero coupling [2]. We see that the true expansion parameter is \hat{g}^2 , and the alternatively normalized action (15) makes it clear that the theory is unstable for $\hat{g}^2 < 0$. Thus we write

$$\frac{\beta(\hat{g})}{\hat{g}} \equiv A(\hat{g}^2) = \int_0^\infty \frac{dz}{\hat{g}^2} B(z) \exp \frac{-z}{\hat{g}^2}. \quad (83)$$

For the perturbation series

$$A(\hat{g}^2) = \sum_{n=1}^{\infty} A_n \hat{g}^{2n}, \quad (84)$$

the Borel transform is

$$B(z) = \sum_{n=1}^{\infty} \frac{A_n}{n!} z^n. \quad (85)$$

In our case,

$$B(z) = \frac{z}{32\pi} - \frac{z^2}{4096\pi^2} + O(z^3). \quad (86)$$

The Borel transform often has poles on the negative real axis associated with instantons [2], but $\beta(\hat{g})$ is well-defined from Eq. (83) as long as $B(z)$ is regular on the positive real axis. A simple and suitable rational (Padé) approximant to $B(z)$ is

$$B(z) \simeq \frac{z}{32\pi + yz} \quad (y \geq 0); \quad (87)$$

fortunately, the choice $y = \frac{1}{4}$ agrees with Eq. (86). We thus take

$$B(z) \simeq \frac{4z}{128\pi + z}, \quad (88)$$

but we do not here attempt to study the possible instanton solutions corresponding to the pole at $z = -128\pi$. Eq. (83) then gives precisely the desired asymptotic behavior

$$\beta(\hat{g}) \simeq 4\hat{g} \quad (\hat{g} \rightarrow \infty). \quad (89)$$

We now ask whether the observed $k^{-5/3}$ energy spectrum (72) is consistent with our theory, although we are unable to derive it systematically. We conjecture that strong-coupling effects produce the spectrum

$$E(k) \sim \mathcal{E}^{2/3} k^{-5/3} \quad (90)$$

for

$$k \gtrsim k_{\text{fr}} = \mathcal{E}^{-1/2} \rho^{3/2}. \quad (91)$$

From Eq. (80), the running coupling is

$$\hat{g}(\Lambda) \sim \mathcal{E}^{-1} \Lambda^4. \quad (92)$$

For nonperturbative effects to be operative down to the wavenumber k_{fr} , we must have

$$\hat{g}(k_{\text{fr}}) \sim (\mathcal{E}^{-1} \rho^2)^3 \gtrsim 1. \quad (93)$$

In the borderline case where $\hat{g}(k_{\text{fr}}) \sim 1$, we have $k_{\text{fr}} \sim \mathcal{E}^{1/4} \sim \rho^{1/2}$, and we can match Eq. (90) in order of magnitude with the perturbative energy spectrum (59):

$$E(k_{\text{fr}}) \sim \mathcal{E}^{2/3} k_{\text{fr}}^{-5/3} \sim \mathcal{E}^{1/4} \sim \frac{k_{\text{fr}}^3}{\rho + k_{\text{fr}}^2}. \quad (94)$$

Even when $\hat{g}(k_{\text{fr}}) \gg 1$, we may guess from Eq. (59) that in order of magnitude

$$E(k_{\text{fr}}) \sim \frac{k_{\text{fr}}^3}{\rho \hat{g}(k_{\text{fr}}) + k_{\text{fr}}^2} \sim \mathcal{E}^{3/2} \rho^{-5/2}, \quad (95)$$

and this again matches Eq. (90) at k_{fr} .

In the case $\hat{g}(k_{\text{fr}}) \gg 1$, the running coupling eventually becomes ~ 1 at a lower wavenumber

$$k_g \sim \mathcal{E}^{1/4}, \quad (96)$$

below which perturbation theory is applicable and the energy spectrum is given roughly by Eq. (60). Thus we envision a varied but continuous behavior of the energy spectrum in the different regions:

$$E(k) \sim \begin{cases} \rho^{-1} k^3 & (k \lesssim \mathcal{E}^{1/4}), \\ \mathcal{E} \rho^{-1} k^{-1} & (\mathcal{E}^{1/4} \lesssim k \lesssim \mathcal{E}^{-1/2} \rho^{3/2}), \\ \mathcal{E}^{2/3} k^{-5/3} & (k \gtrsim \mathcal{E}^{-1/2} \rho^{3/2}). \end{cases} \quad (97)$$

As a further check, we note that the contribution to the energy dissipation rate (79) for each of the three regions is $\sim \mathcal{E}$ (up to a logarithmic factor for the middle region). This suggests that a fully developed stationary inverse cascade has several distinct dissipation ranges. Testing by experiments and simulations is not straightforward, because finite-size effects may become important before the lower-wavenumber ranges are reached.

C. Energy flux and third moment

We have described the ideal inverse cascade in terms of external forcing confined to high wavenumbers (assumed in Sec. IIB) and energy dissipation practically confined to low wavenumbers (made plausible in Secs. III C and V B). This separation is equivalent to the conventional criterion of an inertial range with a constant energy flux. However, unlike the energy spectrum (a simple correlation function), the energy flux in wavenumber space is not invariant under the RG flow and is not given straightforwardly by our local field theory. Renormalization introduces the forcing (77), which is nonzero even

for wavenumbers in the inertial range and so makes the flux appear nonconstant. This effective forcing simply represents the energy transfer from wavenumbers $k > \Lambda$ that have been integrated out.

We can resolve the flux problem by working instead in physical space, where the effective forcing is a differentiated delta function that is zero at finite distances, including the inertial range of lengths. Thus we inquire whether the physical-space energy flux [3]

$$\varepsilon(r) = -\frac{1}{4}\nabla_{\mathbf{r}} \cdot \langle |\delta\mathbf{v}(\mathbf{r})|^2 \delta\mathbf{v}(\mathbf{r}) \rangle \quad (98)$$

is preserved under renormalization. The flux is given in terms of the third moment of the velocity increment

$$\delta\mathbf{v}(\mathbf{r}) = \mathbf{v}(\mathbf{x} + \mathbf{r}) - \mathbf{v}(\mathbf{x}) \quad (99)$$

and is independent of \mathbf{x} by homogeneity. Under stationary conditions, the Navier–Stokes equation (1) yields [32]

$$\begin{aligned} \varepsilon(r) &= (\nu\nabla_{\mathbf{r}}^2 - \alpha)\langle \mathbf{v}(\mathbf{x}) \cdot \mathbf{v}(\mathbf{x} + \mathbf{r}) \rangle + \frac{1}{2}\hat{C}(r) \\ &= [\hat{g}(\Lambda)^{-1}\nabla_{\mathbf{r}}^2 - \rho]\langle \mathbf{v}(\mathbf{x}) \cdot \mathbf{v}(\mathbf{x} + \mathbf{r}) \rangle, \end{aligned} \quad (100)$$

where $\hat{C}(r)$ is the vanishing physical-space force correlation, and we have used Eqs. (75) and (76).

The right-hand side of Eq. (100) can be interpreted as minus the rate of energy dissipation at length scales larger than r . Since $\langle \mathbf{v}(\mathbf{x}) \cdot \mathbf{v}(\mathbf{x} + \mathbf{r}) \rangle$ is an RG-invariant correlation function, only the viscosity $\hat{g}(\Lambda)^{-1}$ introduces cutoff dependence. In accordance with our argument in Sec. VB, as long as the energy dissipation is dominated by friction, the dissipation rate is independent of Λ , giving a well-defined energy flux

$$\varepsilon(r) = -\rho\langle \mathbf{v}(\mathbf{x}) \cdot \mathbf{v}(\mathbf{x} + \mathbf{r}) \rangle \quad (101)$$

proportional to the Fourier transform of the energy spectrum. And if this spectrum is almost entirely concentrated at low wavenumbers $k \lesssim k_{\text{fr}}$, it follows that in the inertial range ($r \ll k_{\text{fr}}^{-1}$) the flux is constant,

$$\varepsilon(r) \simeq \varepsilon(0) = -\rho\langle v^2 \rangle = -\mathcal{E}. \quad (102)$$

D. Intermittency

A striking feature observed in the inverse cascade is the approximate scale invariance of inertial-range velocity correlations (structure functions). The $k^{-5/3}$ energy spectrum (72) gives for the second moment [3]

$$\langle |\delta\mathbf{v}(\mathbf{r})|^2 \rangle \propto \mathcal{E}^{2/3} r^{2/3}, \quad (103)$$

and the constant energy flux (98) gives for the third moment [32]

$$\langle |\delta\mathbf{v}(\mathbf{r})|^2 \delta\mathbf{v}(\mathbf{r}) \rangle \propto \mathcal{E}\mathbf{r}. \quad (104)$$

In our field theory, since the anomalous dimensions vanish, such moments can be written in the form

$$\langle (\delta v)^n \rangle = r^{-n} f_n(\hat{g}(r^{-1}), \rho r^2), \quad (105)$$

where r^{-n} is the kinematic scaling and f_n is a function of the dimensionless running couplings. Eq. (105) should reduce to the observed forms in the inertial range

$$r \ll k_{\text{fr}}^{-1} = \mathcal{E}^{1/2} \rho^{-3/2}, \quad (106)$$

subject to the condition for a fully developed cascade,

$$\hat{g}(k_{\text{fr}}) \sim (\mathcal{E}^{-1} \rho^2)^3 \gg 1. \quad (107)$$

Conditions (106) and (107) are equivalent to

$$(\rho r^2)^{-2} \ll \hat{g}(r^{-1}) \ll (\rho r^2)^{-3}. \quad (108)$$

To achieve complete scale invariance of inertial-range structure functions (absence of intermittency), we must have

$$f_n(\hat{g}(r^{-1}), \rho r^2) \propto \hat{g}(r^{-1})^{-n/3} \quad (109)$$

for the range of arguments (108); then $f_n \propto \mathcal{E}^{n/3} r^{4n/3}$, and

$$\langle (\delta v)^n \rangle \propto \mathcal{E}^{n/3} r^{n/3}. \quad (110)$$

Eq. (109) requires a specific nonperturbative behavior of velocity correlations at strong coupling, mimicking the effect of an anomalous dimension. RG theory alone does not constrain the functions f_n . The well-established second moment (103) and third moment (104) strongly suggest that an exact calculation in our theory would yield the required behavior of f_2 and f_3 . But in the absence of a field-theoretic reason why Eq. (109) should persist for $n \geq 4$, high-order structure functions may generically be expected to violate scale invariance and produce intermittency. In sum, we would not be at all surprised by observations of intermittency in the inverse cascade, but a seeming total absence of intermittency would raise questions about unknown properties of our theory that enforce effective scale invariance.

Some numerical studies of higher moments [4, 5] deal with a nonstationary inverse cascade and find no signs of intermittency. Such results are not directly relevant to this paper but have been explained theoretically [6] based on the growth of the inertial range with time. For the stationary inverse cascade, laboratory experiments [9, 33] reveal no evidence of intermittency. The results of stationary numerical simulations, however, are mixed: A study using linear friction [8] confirms the absence of intermittency, but a study using hypofriction with one inverse Laplacian [7] obtains intermittency that is described as strong and as similar to that observed in the three-dimensional direct cascade. Surprisingly, results from the latter simulation are also presented in a subsequent paper [33] where the intermittency is described as insignificant. The evidence on intermittency in the stationary inverse cascade is unclear, and further numerical studies would be useful to resolve the question. Results exhibiting strong intermittency are most natural, from the viewpoint of our field theory.

The mild hypofriction used in the numerical study obtaining strong intermittency [7] is unlikely to alter the qualitative structure of our theory. While the inverse Laplacian renders the initial Navier–Stokes equation (1) nonlocal, the differentiated form (4) and the field-theory action (18) are still local in terms of the stream function ψ . The hypofriction term certainly violates Galilean invariance, but this symmetry holds for zero hypofriction and so its implications for the RG functions persist in minimal subtraction even when hypofriction is added. The same arguments used for linear friction in this paper suggest that intermittency should be expected with hypofriction as well. It would be interesting to perform a direct numerical study of the effect of modified friction on intermittency in the stationary inverse cascade.

VI. GENERALIZED BURGERS EQUATION

A. Dimensional continuation

As an example of an alternative statistical fluid model to which our RG methods can be applied but which exhibits different behavior, let us briefly consider the one-dimensional Burgers equation [34]

$$\dot{v} + v\nabla v - \nu\nabla^2 v + \alpha v = f. \quad (111)$$

Here v is the velocity field of a fluid without pressure, f is the force per unit mass, ν is the kinematic viscosity, and α is the friction coefficient (not normally included in the Burgers equation but useful in controlling the long-distance behavior). As with the two-dimensional incompressible fluid, we assume that the forcing is confined to a band of high wavenumbers, and we study the response at lower wavenumbers.

FNS [12] found that the UV-stirred Burgers equation, like the Navier–Stokes equation, has a dimensionless coupling in two spatial dimensions and can be analyzed by an ϵ -expansion in $d = 2 - \epsilon$. But their continuation of the Burgers equation to $d > 1$ does not preserve important one-dimensional properties, and their ϵ -expansion is not fully consistent [12, 34]. With $\nu = \alpha = f = 0$, Eq. (111) yields conservation of the “energy”

$$E = \frac{1}{2} \int dx v^2. \quad (112)$$

This E is not proportional to the physical energy of a pressure-free fluid, because it does not account for the varying density; nevertheless, E is conserved in $d = 1$, and leads to a fluctuation-dissipation theorem (FDT). It is not easy, however, to generalize Eq. (111) to $d > 1$ so that a similar “energy” is conserved, while maintaining other key properties such as Galilean invariance. This is the task we now address.

If we neglect dissipation and forcing, the conservation of E in $d = 1$ follows from the relation

$$0 = v\dot{v} + \frac{1}{3}\nabla(v^3) \equiv v(\dot{v} + v\nabla v). \quad (113)$$

The analogue in $d > 1$ that would yield conservation of

$$E = \frac{1}{2} \int d^d x |\mathbf{v}|^2 \quad (114)$$

is

$$\begin{aligned} 0 &= \mathbf{v} \cdot \dot{\mathbf{v}} + A\nabla \cdot (v^2 \mathbf{v}) \\ &\equiv \mathbf{v} \cdot [\dot{\mathbf{v}} + A(\nabla \cdot \mathbf{v})\mathbf{v} + (A - B)\nabla(v^2) + 2B(\mathbf{v} \cdot \nabla)\mathbf{v}] \\ &\equiv \mathbf{v} \cdot \mathbf{w}. \end{aligned} \quad (115)$$

Unfortunately, whatever the choice of the constants A and B , the quantity \mathbf{w} is not Galilean covariant and is not a suitable generalization of $(\dot{v} + v\nabla v)$.

To remedy this problem, we impose the potential-flow condition

$$\mathbf{v} = \nabla\psi, \quad (116)$$

as is commonplace when considering a multidimensional Burgers equation. Then, because

$$\dot{E} = \int d^d x \mathbf{v} \cdot \mathbf{w} = \int d^d x \psi(-\nabla \cdot \mathbf{w}), \quad (117)$$

a scalar equation of motion can conserve

$$E = \frac{1}{2} \int d^d x \nabla_i \psi \nabla_i \psi. \quad (118)$$

We take

$$\begin{aligned} 0 = -\nabla \cdot \mathbf{w} &\equiv -\nabla^2 \dot{\psi} - A\nabla^2 \psi \nabla^2 \psi - 2A\nabla_i \nabla_j \psi \nabla_i \nabla_j \psi \\ &\quad - 3A\nabla_i \psi \nabla_i \nabla^2 \psi. \end{aligned} \quad (119)$$

If $A = \frac{1}{3}$, this expression is covariant under the Galilean transformation

$$\psi(t, \mathbf{x}) \rightarrow \psi(t, \mathbf{x} + \mathbf{u}t) - \mathbf{u} \cdot \mathbf{x}, \quad (120)$$

which induces

$$\mathbf{v}(t, \mathbf{x}) \rightarrow \mathbf{v}(t, \mathbf{x} + \mathbf{u}t) - \mathbf{u}. \quad (121)$$

Upon restoring dissipation and forcing, we therefore propose

$$\begin{aligned} &-\nabla^2 \dot{\psi} - \nabla_i \psi \nabla_i \nabla^2 \psi - \frac{1}{3} \nabla^2 \psi \nabla^2 \psi \\ &- \frac{2}{3} \nabla_i \nabla_j \psi \nabla_i \nabla_j \psi + \nu \nabla^4 \psi - \alpha \nabla^2 \psi = \eta \end{aligned} \quad (122)$$

as a fully satisfactory multidimensional Burgers equation that reduces to Eq. (111) in $d = 1$. Eq. (122) is formally very similar to the incompressible stream-function equation (4), and we will follow our previous analysis closely.

B. One-loop renormalization

As in Sec. II, we assume Gaussian forcing and introduce a path integral with the action

$$\begin{aligned}
S &= \int dt d^d x \left[\frac{1}{2} (-\nabla^2 p) D(-\nabla^2) p \right. \\
&\quad \left. + ip(-\nabla^2 \psi - \nabla_i \psi \nabla_i \nabla^2 \psi - \frac{1}{3} \nabla^2 \psi \nabla^2 \psi \right. \\
&\quad \left. - \frac{2}{3} \nabla_i \nabla_j \psi \nabla_i \nabla_j \psi + \nu \nabla^4 \psi - \alpha \nabla^2 \psi) \right] \\
&= \int dt d^d x \left[\frac{1}{2} (-\nabla^2 p) D(-\nabla^2) p + i\nu p \nabla^4 \psi - i\alpha p \nabla^2 \psi \right. \\
&\quad \left. - ip \nabla^2 \psi - i \nabla_i \nabla_j p \left(\frac{1}{6} \delta_{ij} \nabla_k \psi \nabla_k \psi + \frac{1}{3} \nabla_i \psi \nabla_j \psi \right) \right], \tag{123}
\end{aligned}$$

where we have again integrated the $p\psi\psi$ term by parts. Analysis of dimensions in $d = 2 - \epsilon$ proceeds as before, since all terms contain the same numbers of derivatives as for the incompressible fluid. The final Burgers action, to be compared with Eq. (18), is

$$\begin{aligned}
S &= \int dt d^d x \left[\frac{1}{2} g^{-1} \nabla^2 p \nabla^2 p + ig^{-1} p \nabla^4 \psi - i\rho p \nabla^2 \psi \right. \\
&\quad \left. - ip \nabla^2 \psi - i \nabla_i \nabla_j p \left(\frac{1}{6} \delta_{ij} \nabla_k \psi \nabla_k \psi + \frac{1}{3} \nabla_i \psi \nabla_j \psi \right) \right]. \tag{124}
\end{aligned}$$

The scaling dimensions are again given by Eq. (20).

The only change to the Feynman rules in Fig. 1 is the vertex factor, which now becomes

$$-\Gamma_0^{\psi\psi p} = \frac{1}{3} i |\mathbf{k}_1 + \mathbf{k}_2|^2 \mathbf{k}_1 \cdot \mathbf{k}_2 + \frac{2}{3} i (k_1^2 + \mathbf{k}_1 \cdot \mathbf{k}_2) (k_2^2 + \mathbf{k}_1 \cdot \mathbf{k}_2). \tag{125}$$

Thanks to conservation of the “energy” E , the FDT is obtained just as in Sec. III B, and together with Galilean invariance it implies that the anomalous dimensions vanish. Thus, to find the new one-loop β function, we need only recompute one of the diagrams in Fig. 2. We calculate

$$\Gamma_1^{\psi p} = igq^4 \left(\frac{1}{32\pi\epsilon} - \frac{\ln(g\rho/4\pi) + \gamma_E + \frac{8}{9}}{64\pi} + O(\epsilon) \right), \tag{126}$$

to be compared with Eq. (30). Curiously, the $O(\epsilon^{-1})$ term is exactly the same and again leads to the one-loop β function

$$\beta(\bar{g}) = -\frac{1}{2} \epsilon \bar{g} + \frac{\bar{g}^3}{32\pi} + O(\bar{g}^5). \tag{127}$$

But the $O(\epsilon^0)$ term in Eq. (126), which would enter a calculation of the two-loop β function, differs from Eq. (30), and we have no reason to expect an identity between the β functions beyond one loop.

Our multidimensional Burgers equation (122) appears not to have been investigated previously, and it is possible that numerical simulations in two or three dimensions could reveal interesting and unexpected behavior. The focus here, however, is on the extrapolation to one

dimension ($\epsilon = 1$), where we seek to explain the known behavior [34] of the ordinary Burgers equation (111). If ϵ is positive and small, then the β function (127) has a nontrivial IR-stable fixed point at

$$\bar{g}_*^2 = 16\pi\epsilon + O(\epsilon^2). \tag{128}$$

By contrast, when a simpler continuation of the Burgers equation was used, the fixed point appeared to be IR-unstable near two dimensions [12, 34]. From our results it is natural to expect an IR-stable strong-coupling fixed point in one dimension ($\epsilon = 1$).

C. Comparison with inverse-cascade model

Due to the nontrivial fixed point, the response of the one-dimensional Burgers equation to UV forcing is different from that of the two-dimensional Navier–Stokes equation—even in the absence of friction. At wavenumbers low enough that the fixed point is reached, Burgers correlation functions (at equal or unequal times) exhibit purely kinematic scaling, since all anomalous dimensions vanish. For example, from Eq. (20), the scaling of time and frequency is given by

$$d_t = -2 + \frac{1}{2}\epsilon = -\frac{3}{2}, \quad \omega \propto k^{3/2}. \tag{129}$$

Meanwhile, in both models, the FDT implies that the energy spectrum (an equal-time correlation function) obeys equipartition. These conclusions agree with previous analytic [12] and numerical [34] studies of the frictionless one-dimensional Burgers equation.

We have argued that the inclusion of friction dramatically alters the behavior of the two-dimensional Navier–Stokes model, from equipartition to a stationary inverse cascade. This is plausible only in the presence of a large, rapidly flowing coupling \hat{g} . We noted in Sec. V how this RG flow could give rise to a constant energy flux and a $k^{-5/3}$ spectrum. No such profound effect is expected for friction in the one-dimensional Burgers equation. Correlation functions will be modified at very low wavenumbers $\lesssim \rho^{2/3}$, but as long as \hat{g} remains close to the fixed point, higher wavenumbers will retain the equipartition spectrum.

An open question concerns the strong-coupling behavior of our generalized Burgers equation (122) in two dimensions with friction. If the β function happens to grow asymptotically in the same way as the Navier–Stokes one, then the arguments of Sec. V can be repeated and it is at least possible that this Burgers model could exhibit an inverse energy cascade. If true, this should also be evident if the equation is studied numerically. It is unclear, however, whether this multidimensional Galilean-invariant scalar field theory has a direct physical application.

VII. DISCUSSION

We have presented a statistical field theory capable of describing the stationary inverse energy cascade in two-dimensional incompressible turbulence, and computed the RG functions through two loops. By contrast with previous RG studies of turbulence, we have taken advantage of the nature of the inverse cascade, with external forcing confined to high wavenumbers, to work with a conventional local field theory. The consequences of Galilean invariance and the fluctuation-dissipation theorem have been systematically derived based on the underlying symmetries of the action. After taking these symmetries into account, we have evaluated the necessary two-loop diagrams in dimensional regularization to obtain the two-loop β function

$$\beta(\bar{g}) = \frac{\bar{g}^3}{32\pi} - \frac{\bar{g}^5}{2048\pi^2} + O(\bar{g}^7), \quad (130)$$

which is independent of the renormalization scheme to precisely this order.

Because the anomalous dimensions vanish identically in minimal subtraction, no RG fixed point can yield the observed $k^{-5/3}$ energy spectrum of the inverse cascade. Instead, we have found that the inverse cascade could plausibly arise from nonperturbative strong-coupling effects in the presence of friction. The apparent anomalous dimension of the velocity must arise from the rapid RG flow of the coupling. Cutoff independence of the energy dissipation rate (or constancy of the energy flux) requires the strong-coupling behavior

$$\beta(\hat{g}) \simeq 4\hat{g} \quad (\hat{g} \rightarrow \infty), \quad (131)$$

and we have also obtained this in a heuristic way from a Borel transformation of the two-loop β function. The observed energy spectrum in the inertial range has been

matched with perturbative results at the wavenumbers where dissipation becomes important. Inertial-range intermittency (violation of scale invariance) is generically expected because the coupling flows rapidly with scale, but the evidence on intermittency from numerical simulations is mixed. On the other hand, a similar RG analysis of the one-dimensional Burgers equation confirms the simpler behavior of that model, controlled by a strong-coupling fixed point.

Our greatest difficulty is that the inverse cascade appears to be intrinsically a nonperturbative phenomenon. To make quantitative predictions, such as the exponent of the energy spectrum or the value of the Kolmogorov constant, it may be useful to combine a high-order perturbative calculation with an appropriate resummation method, as in our analysis of the strong-coupling β function. Of course evaluating additional diagrams with two or more loops will be very challenging, especially if the finite parts are needed. At the present stage, the most intriguing prediction of our theory is that substantial intermittency should be expected in the stationary inverse cascade. It would be helpful to have more robust and consistent results from experiments and simulations to determine whether this expectation is realized, and if it is not, to identify the field-theoretic explanation.

Acknowledgments

I thank A. M. Polyakov, S. L. Sondhi, H. L. Verlinde, and V. Yakhot for helpful discussions.

This material is based upon work supported by the National Science Foundation under Grant No. 0243680. Any opinions, findings, and conclusions or recommendations expressed in this material are those of the author and do not necessarily reflect the views of the National Science Foundation.

-
- [1] R. H. Kraichnan, *Phys. Fluids* **10**, 1417 (1967).
 - [2] J. Zinn-Justin, *Quantum Field Theory and Critical Phenomena* (Oxford University Press, Oxford, 1996), 3rd ed.
 - [3] U. Frisch, *Turbulence: The Legacy of A. N. Kolmogorov* (Cambridge University Press, Cambridge, 1995).
 - [4] L. M. Smith and V. Yakhot, *Phys. Rev. Lett.* **71**, 352 (1993).
 - [5] L. M. Smith and V. Yakhot, *J. Fluid Mech.* **274**, 115 (1994).
 - [6] V. Yakhot, *Phys. Rev. E* **60**, 5544 (1999).
 - [7] A. Babiano, B. Dubrulle, and P. Frick, *Phys. Rev. E* **52**, 3719 (1995).
 - [8] G. Boffetta, A. Celani, and M. Vergassola, *Phys. Rev. E* **61**, R29 (2000).
 - [9] J. Paret and P. Tabeling, *Phys. Fluids* **10**, 3126 (1998).
 - [10] J. Honkonen, *Phys. Rev. E* **58**, 4532 (1998).
 - [11] A. M. Polyakov, *Nucl. Phys. B* **396**, 367 (1993).
 - [12] D. Forster, D. R. Nelson, and M. J. Stephen, *Phys. Rev. A* **16**, 732 (1977).
 - [13] C. DeDominicis and P. C. Martin, *Phys. Rev. A* **19**, 419 (1979).
 - [14] L. Ts. Adzhemyan, N. V. Antonov, and A. N. Vasiliev, *The Field Theoretic Renormalization Group in Fully Developed Turbulence* (Gordon and Breach, Amsterdam, 1999).
 - [15] M. Lesieur, *Turbulence in Fluids* (Kluwer, Boston, 1997), 3rd ed.
 - [16] G. 't Hooft and M. Veltman, *Nucl. Phys. B* **44**, 189 (1972).
 - [17] P. C. Martin, E. D. Siggia, and H. A. Rose, *Phys. Rev. A* **8**, 423 (1973).
 - [18] R. Bausch, H. K. Janssen, and H. Wagner, *Z. Phys. B* **24**, 113 (1976).
 - [19] R. Phythian, *J. Phys. A* **10**, 777 (1977).
 - [20] L. D. Adzhemyan, A. N. Vasil'ev, and Yu. M. Pis'mak, *Theor. Math. Phys. (USSR)* **57**, 1131 (1983).

- [21] G. 't Hooft, Nucl. Phys. B **61**, 455 (1973).
- [22] U. Decker and F. Haake, Phys. Rev. A **11**, 2043 (1975).
- [23] E. Frey and U. C. Täuber, Phys. Rev. E **50**, 1024 (1994).
- [24] L. Ts. Adzhemyan, N. V. Antonov, M. V. Kompaniets, and A. N. Vasil'ev, Int. J. Mod. Phys. B **17**, 2137 (2003).
- [25] S. Wolfram, *The Mathematica Book* (Cambridge University Press, Cambridge, 1999), 4th ed.
- [26] W. H. Press, S. A. Teukolsky, W. T. Vetterling, and B. P. Flannery, *Numerical Recipes in C: The Art of Scientific Computing* (Cambridge University Press, Cambridge, 1992), section 7.8, 2nd ed.
- [27] U. Frisch and P. L. Sulem, Phys. Fluids **27**, 1921 (1984).
- [28] S. Danilov and D. Gurarie, Phys. Rev. E **63**, 020203(R) (2001).
- [29] J. Sommeria, J. Fluid Mech. **170**, 139 (1986).
- [30] M. E. Maltrud and G. K. Vallis, J. Fluid Mech. **228**, 321 (1991).
- [31] V. Borue, Phys. Rev. Lett. **72**, 1475 (1994).
- [32] D. Bernard, Phys. Rev. E **60**, 6184 (1999).
- [33] T. Dubos, A. Babiano, J. Paret, and P. Tabeling, Phys. Rev. E **64**, 036302 (2001).
- [34] V. Yakhot and Z.-S. She, Phys. Rev. Lett. **60**, 1840 (1988).